# Solid-state dye-sensitized mesoporous $TiO_2$ solar cells with high photon-to-electron conversion efficiencies

**U. Bach*, D. Lupo†‡, P. Comte*, J. E. Moser*, F. Weissörtel§, J. Salbeck§, H. Spreitzer† & M. Grätzel***

** Institute of Photonics and Interfaces, Swiss Federal Institute of Technology, CH-1015 Lausanne, Switzerland*

*† Hoechst Research & Technology Deutschland GmbH & Co. KG, Industriepark Höchst, D-65926 Frankfurt, Germany*

*§ Max-Planck-Institut für Polymerforschung, D-55128 Mainz, Germany*

**Solar cells based on dye-sensitized mesoporous films of $TiO_2$ are low-cost alternatives to conventional solid-state devices[1]. Impressive solar-to-electrical energy conversion efficiencies have been achieved with such films when used in conjunction with liquid electrolytes[2]. Practical advantages may be gained by the replacement of the liquid electrolyte with a solid charge-transport material. Inorganic p-type semiconductors[3,4] and organic materials[5–9] have been tested in this regard, but in all cases the incident monochromatic photon-to-electron conversion efficiency remained low. Here we describe a dye-sensitized heterojunction of $TiO_2$ with the amorphous organic hole-transport material 2,2′,7,7′-tetrakis(*N*,*N*-di-*p*-methoxyphenyl-amine)9,9′-spirobifluorene (OMeTAD; refs. 10 and 11). Photoinduced charge-carrier generation at the heterojunction is very efficient. A solar cell based on OMeTAD converts photons to electric current with a high yield of 33%.**

The hole conductor contains a spiro-centre (a tetrahedral carbon linking two aromatic moieties) which is introduced in order to improve the glass-forming properties and prevent crystallization of the organic material. Its glass transition temperature of $T_g = 120\,°C$, measured by differential scanning calorimetry, is much higher then that of the widely used hole conductor TPD (*N*,*N*′-diphenyl-*N*,*N*′-bis(3-methylphenyl)4,4′-diamine; $T_g = 62\,°C$). Crystallization is undesirable as it would impair the formation of a good contact between the mesoporous surface of the $TiO_2$ and the hole conductor. The methoxy groups are introduced in order to match the oxidation potential of the hole-transport medium (HTM) to that of the sensitizer $Ru(II)L_2(SCN)_2$ (where L is 4,4′-dicarboxy-2,2′-bipyridyl), used in this study.

Figure 1 shows a scheme for the electron-transfer processes occurring at the dye-sensitized heterojunction. Visible-light absorption by the sensitizer is followed by electron transfer to the conduction band of $TiO_2$. The dye is regenerated by hole injection into the HTM. The $TiO_2$ conduction-band electrons, as well as the holes in the HTM, are subsequently transported by electronic conduction to the contact electrodes. Pulsed nanosecond laser photolysis was used in conjunction with time-resolved absorption spectroscopy to scrutinize the dynamics of the photoinduced charge separation process. Figure 2 shows the transient absorption spectrum of a dye-sensitized mesoporous $TiO_2$ film in the absence and presence of OMeTAD, measured 50 ns after laser excitation. In the absence of OMeTAD, dye bleaching at ~500 nm is observed and a broad positive transient absorption appears above 600 nm due to the absorption of the oxidized dye $Ru(III)L_2(SCN)_2^+$ and of the $TiO_2$ conduction-band electrons. Electron injection proceeds in the femtosecond domain[12], while the subsequent recapture of injected electrons by the oxidized dye takes several microseconds. In the presence of OMeTAD, the bleaching signal disappears. Instead, the transient absorption rises vertically within the laser pulse. Comparison of the transient spectra obtained in the presence of OMeTAD with the absorption band of chemically oxidized OMeTAD confirms that the species giving rise to the new spectral feature is the radical cation $OMeTAD^+$. Apparently, electron injection from the excited sensitizer into $TiO_2$ is immediately followed by regeneration of the dye via hole transfer to OMeTAD, as shown below:

$$Ru(II)L_2(SCN)_2^* \rightarrow Ru(III)L_2(SCN)_2^+ + e^-(TiO_2) \quad (1)$$

$$OMeTAD + Ru(III)L_2(SCN)_2^+ \rightarrow Ru(II)L_2(SCN)_2 + OMeTAD^+ \quad (2)$$

The process shown in equation (2) was too fast to be monitored with the laser equipment employed, setting an upper limit of 40 ns for the hole-transfer time.

A blank experiment was performed using mesoporous $Al_2O_3$ films instead of $TiO_2$ as a support for the $Ru(II)L_2(SCN)_2$ sensitizer; the results showed that hole transfer from the excited state of the dye

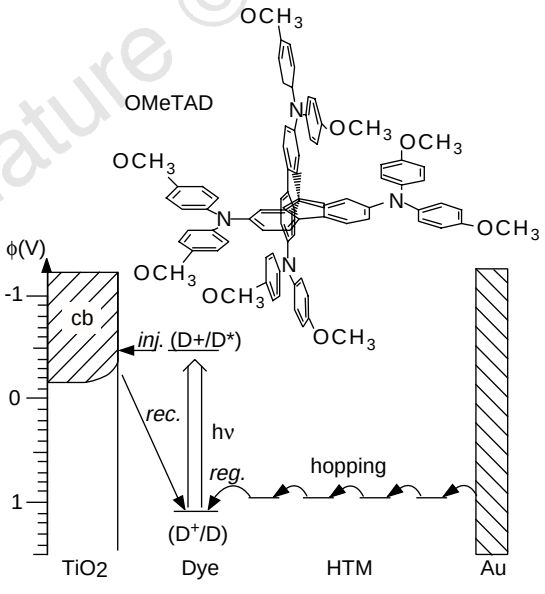


**Figure 1** Scheme for the electron-transfer processes (inj., injection; reg., regeneration; rec., recapture; hopping) occurring in the dye-sensitized heterojunction. Also shown are the approximate redox potentials and band energies of the different components.

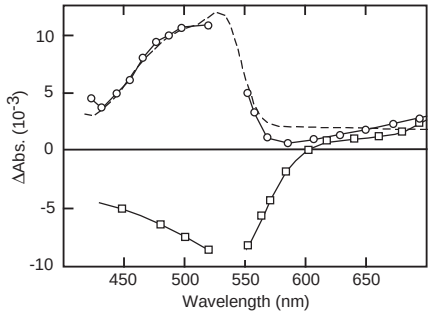


**Figure 2** Absorption spectra from time-resolved laser photolysis experiments. Shown are the transient absorption spectra of a dye-sensitized mesoporous $TiO_2$ film in the absence (squares, contact medium propylene carbonate) and in the presence (circles) of solid OMeTAD, 50 ns after excitation at 532 nm. For comparison, the absorption spectrum of chemically oxidized OMeTAD in chlorobenzene:acetonitrile = 90:10 is also shown (dashed line, arbitrary units).

‡ Present address: Materials Science Laboratories, Sony International (Europe) GmbH, Stuttgarter Strasse 106, 70736 Fellbach, Germany.

to the OMeTAD does not contribute significantly to the photo-induced charge-separation phenomena observed.

The photovoltaic performance of the dye-sensitized heterojunction was studied by means of sandwich-type cells, shown schematically in Fig. 3a. The working electrode consisted of conducting glass (F-doped $SnO_2$, sheet resistance 10 Ω per square) onto which a compact $TiO_2$ layer was deposited by spray pyrolysis[13]. This avoids direct contact between the HTM layer and the $SnO_2$ which would short-circuit the cell. A 4.2-μm-thick mesoporous film of $TiO_2$ was deposited by screen printing onto the compact layer[14], and derivatized with $Ru(II)L_2(SCN)_2$ by adsorption from acetonitrile. The HTM was introduced into the mesopores by spin-coating a solution of OMeTAD in chlorobenzene onto the $TiO_2$ film, and subsequent evaporation of the solvent. A semi-transparent gold back contact was evaporated on top of the hole conductor under vacuum.

Figure 3b shows the photocurrent action spectrum of a typical cell under short-circuit conditions. The given values are not corrected for reflection and absorption losses of the conducting glass, which are estimated to be at least 15% in the visible region of the spectrum. The spectrum closely matches the absorption spectrum of the dye, confirming that the observed photocurrent arises from electron injection by the sensitizer. The maximum value of the incident photo-to-electron conversion efficiency (IPCE) is 33%, which is more than two orders of magnitude larger than the previously reported value for a similar dye-sensitized solid heterojunction[9] and only a factor of ~2 lower than with liquid electrolytes[2].

The coating solution used for the device in Fig. 3b contained 0.33 mM $N(PhBr)_3SbCl_6$ and 15 mM $Li[(CF_3SO_2)_2N]$ in addition to 0.17 M OMeTAD. In the absence of these additives, the maximum IPCE was only 5%. $N(PhBr)_3SbCl_6$ acts as a dopant, introducing free charge carriers in the HTM by oxidation, as confirmed by spectroelectrochemical measurements. Partial oxidation of OMeTAD by $N(PhBr)_3SbCl_6$ is a convenient way to control the dopant level[15]. On adding $N(PhBr)_3SbCl_6$ to a solution of OMeTAD in chlorobenzene, the radical cation $OMeTAD^+$ is instantly formed. The spectral features of $OMeTAD^+$ remained unchanged during solvent evaporation and glass formation, except for a small hypochromic shift. No subsequent absorption changes were detectable over several weeks, confirming the temporal stability of $OMeTAD^+$ in the HTM.

The second additive, $Li[(CF_3SO_2)_2N]$, is a source of $Li^+$ ions, which are known to be potential-determining for $TiO_2$ (ref. 16). Along with the protons from the carboxylic acid groups of $Ru(II)L_2(SCN)_2$, they confer a positive charge on the surface of the oxide. As the sensitizer is negatively charged a local electrostatic field is produced, assisting electron injection into the $TiO_2$ while retarding recapture of the electron by the oxidized dye. The lithium salt may also compensate for space-charge effects. Under light illumination of the heterojunction, a net positive space charge is expected to be formed in the HTM, inducing a local field that impairs current flow. The lithium salt could screen this field, thereby eliminating the space-charge control of the photocurrent. Improvement of the photovoltaic performance of dye-sensitized heterojunctions by immersion in $LiClO_4$ solutions was also reported by Murakoshi *et al.*[5].

Figure 4 shows current-density/voltage curves employing the device structure shown in Fig. 3a. Curves I and II were obtained with hole conductor containing both the $N(PhBr)_3SbCl_6$ dopant and the $Li[(CF_3SO_3)_2N]$ salt, whereas these additives were absent for curve III. Curve I was measured in the dark, whereas II and III were obtained under light illumination. The device that contains the hole conductor without additives performs poorly, the conversion yield being only 0.04% at a white-light illumination of 9.4 mW $cm^{-2}$. Addition of the dopant and $Li^+$ salt increases the overall conversion efficiency to 0.74%. Under full sunlight (100 mW $cm^{-2}$, air mass 1.5), the short-circuit photocurrent density reached 3.18 mA $cm^{-2}$, a value which is unprecedented for solar cells based on organic solids. Further improvement of the photovoltaic performance is expected, as many parameters of the cell assembly have not yet been optimized. Preliminary stability tests performed over 80 h using the visible output of a 400 W Xe lamp showed that the photocurrent was stable within ±20%, while the open-circuit voltage and the fill factor (see Methods) increased. The total charge passed through the cell during illumination was 300 C $cm^{-2}$; corresponding to turnover numbers of about 8,400 and 60,000 for the OMeTAD and the dye, respectively. This shows that the hole conductor can sustain photovoltaic operation without significance degradation.

From the present findings, the concept of dye-sensitized heterojunctions emerges as a very interesting and viable option for future

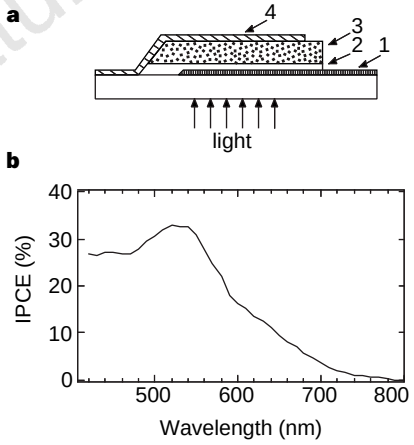


**Figure 3** Structure and spectral response of the photovoltaic devices. **a**, Structure 1, conducting F-doped $SnO_2$-coated glass; 2, compact $TiO_2$ layer; 3, dye-sensitized heterojunction; 4, gold electrode. **b**, Photocurrent action spectrum for a dye-sensitized heterojunction, the structure of which is shown above. The IPCE value corresponds to the number of electrons generated by monochromatic light in the external circuit, divided by the number of incident photons. The 4.2-μm-thick mesoporous $TiO_2$ film was sensitized with $Ru(II)L_2(SCN)_2$, spin-coated with a solution of 0.17 M OMeTAD, 0.33 mM $N(PhBr)_3SbCl_6$ and 15 mM $Li[(CF_3SO_2)_2N]$ in chlorobenzene with 5% acetonitrile added.

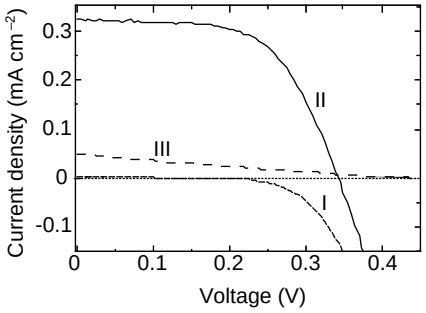


**Figure 4** Current-density/voltage characteristics. Shown are characteristics of the same device as in Fig. 3, obtained in the dark (I) and under white-light illumination at 9.4 mW $cm^{-2}$ (II). The spectral distribution corresponded to global air mass 1.5 corrected for spectral mismatch. The short-circuit current density was 0.32 mA $cm^{-2}$, the open-circuit voltage 342 mV and the fill factor 62% corresponding to an overall conversion efficiency of 0.74%. For comparison, the photocurrent-density/voltage characteristic of a cell containing no $N(PhBr)_3SbCl_6$ or $Li[(CF_3SO_2)_2N]$ is also shown (III).

low-cost solid-state solar cells. Photodiodes based on interpenetrating polymer networks of poly(phenylenevinylene) derivatives[17,18] present a related approach. The main difference to our system is that at least one component of the polymer network needs to function simultaneously as an efficient light absorber and a good charge-transport material. The dye-sensitized heterojunction cell offers a greater flexibility, as the light absorber and charge-transport material can be selected independently to obtain optimum solar-energy harvesting and high photovoltaic output. □

### Methods

**Compounds.** OMeTAD was pure according to $^1$H-NMR and HPLC analysis. The synthesis will be reported elsewhere. $Ru(II)L_2(SCN)_2$ was prepared as previously described[2].

**Transient absorption spectroscopy.** This was carried out with a Nd-YAG laser as excitation light source, producing a 6-ns pulse at 532 nm of typically 1 mJ cm$^{-2}$, with a repetition frequency of 30 Hz. The probe light was provided by a Xe lamp, which was spectrally narrowed by cut-off and interference filters before passing the device. A monochromator combined with a photomultiplier was used as detection system. A Tektronix 524 TDS oscilloscope was used to record and store the data. For the laser experiments, dye-sensitized mesoporous semiconductor films were deposited on ordinary glass.

**Photocurrent-voltage characteristics.** These were measured with a Keithley 2400 Source Meter and a 400 W Xe lamp. A Schott KG3 filter was used in order to approach the spectral distribution of the lamp to air mass 1.5 G. The light intensity was regulated to the desired energy output by using a silicon solar cell, calibrated at the ISE-Fraunhofer Institut in Freiburg Germany. Efficiencies were corrected for the spectral mismatch. The fill factor (FF) is defined as $FF = V_{opt}I_{opt}/I_{sc}V_{oc}$, where $V_{opt}$ and $I_{opt}$ are respectively current and voltage for maximum power output, and $I_{sc}$ and $U_{oc}$ are the short-circuit current and open-circuit voltage, respectively.

Received 8 May; accepted 13 July 1998.


1. O'Regan, B. & Grätzel, M. A low-cost, high-efficiency solar cell based on dye-sensitized colloidal $TiO_2$ films. *Nature* **353,** 737–739 (1991).
2. Nazeeruddin, M. K. *et al*. Conversion of light to electricity by cis-$X_2$bis(2,2′-bipyridyl-4,4′-dicarboxylate)ruthenium(II) charge-transfer sensitizers (X = Cl$^-$,Br$^-$,I$^-$,CN$^-$ and SCN$^-$) on nanocrystalline $TiO_2$ electrodes. *J. Am. Chem. Soc.* **115,** 6382–6390 (1993).
3. O'Regan, B. & Schwarz, D. T. Large enhancement in photocurrent efficiency caused by UV illumination of the dye-sensitized heterojunction $TiO_2$/RuLL′NCS/CuSCN: initiation and potential mechanism. *Chem. Mater.* **10,** 1501–1509 (1998).
4. Tennakone, K., Kumara, G. R. R. A., Kumarasinghe, A. R., Wijayantha, K. G. U. & Sirimanne, P. M. Dye-sensitized nano-porous solid-state photovoltaic cell. *Semicond. Sci. Technol.* **10,** 1689–1693 (1995).
5. Murakoshi, K., Kogure, R. & Yanagida, S. Solid state dye-sensitized $TiO_2$ solar cell with polypyrrole as hole transport layer. *Chem. Lett.* **5,** 471–472 (1997).
6. Bach, U. *et al.* Ultrafast hole injection from dye molecules into an organic hole conductor for dye sensitized solid state solar cells. *Abstract Book, Bayreuth Polymer & Materials Research Symposium*, P28 (Bayreuth, 1997).
7. Weissörtel, F. *Amorphous niedermolekulare Ladungstransportmaterialien für nanokristalline Solarzellen.* Thesis, Univ. Regensburg (1996).
8. Grätzel, M. in *Future Generation Photovoltaic Technologies* Vol. 404 (ed. McConnell, R.) 119–126 (Am. Inst. Phys., Denver, 1997).
9. Hagen, J. *et al.* Novel hybrid solar cells consisting of inorganic nanoparticles and an organic hole transport material. *Synth. Met.* **89,** 215–220 (1997).
10. Salbeck, J., Weissörtel, F. & Bauer, J. Spiro linked compounds for use as active materials in organic light emitting diodes. *Macromol. Symp.* **125,** 121–132 (1997).
11. Salbeck, J., Yu, N., Bauer, J., Weissörtel, F. & Bestgen, H. Low molecular organic glasses for blue electroluminescence. *Synth. Met.* **91,** 209–215 (1997).
12. Tachibana, Y., Moser, J. E., Grätzel, M., Klug, D. R. & Durrant, J. R. Subpicosecond interfacial charge separation in dye-sensitized nanocrystalline titanium dioxide films. *J. Phys. Chem.* **100,** 20056–20062 (1996).
13. Kavan, L. & Grätzel, M. Highly efficient semiconducting $TiO_2$ photoelectrodes prepared by aerosol pyrolysis. *Electrochim. Acta* **40,** 643–652 (1995).
14. Barbé, C. J. *et al.* Nanocrystalline titanium oxide electrodes for photovoltaic applications. *J. Am. Ceram. Soc.* **80,** 3157–3171 (1997).
15. Abkowitz, M. & Pai, D. M. Comparison of the drift mobility measured under transient and steady-state conditions in a prototypical hopping system. *Phil. Mag. B* **53,** 192–216 (1986).
16. Enright, B., Redmond, G. & Fitzmaurice, D. Spectroscopic determination of flat-band potentials for polycrystalline $TiO_2$ electrodes in mixed-solvent systems. *J. Phys. Chem.* **97,** 1426–1430 (1994).
17. Halls, J. J. M. *et al.* Efficient photodiodes from interpenetrating polymer networks. *Nature* **376,** 498–500 (1995).
18. Yu, G., Gao, J., Hummelen, J. C., Wudl, F. & Heeger, A. J. Polymer photovoltaic cells: enhanced efficiencies via a network of internal donor acceptor heterojunctions. *Science* **270,** 1789–1791 (1995).


**Acknowledgement.** This work was supported by the Swiss National Science Foundation and the European Joule III programme (OFES).

Correspondence and requests for materials should be addressed to M.G. (e-mail: michael.graetzel@epfl.ch).

# Accumulation of persistent organochlorine compounds in mountains of western Canada

**Jules M. Blais*†, David W. Schindler*, Derek C. G. Muir†‡, Lynda E. Kimpe§, David B. Donald‖ & Bruno Rosenberg¶**

* *Department of Biological Sciences, University of Alberta, Edmonton, Alberta, Canada T6G 2E9*
‡ *Department of Fisheries and Oceans, Freshwater Institute, 501 University Crescent, Winnipeg, Manitoba, Canada R3T 2N6*
§ *Public Health Sciences, University of Alberta, Edmonton, Alberta, Canada T6G 2G3*
‖ *Environment Canada, Room 300 Park Plaza, 2365 Albert Street, Regina, Saskatchewan, Canada S4P 4K1*
¶ *Freshwater Institute, Winnipeg, Manitoba, Canada R3T 2N6*

**Persistent, semi-volatile organochlorine compounds, including toxic industrial pollutants and agricultural pesticides, are found everywhere on Earth, including in pristine polar and near-polar locations[1–4]. Higher than expected occurrences of these compounds in remote regions are the result of long-range transport in the atmosphere, precipitation and 'cold condensation'—the progressive volatilization in relatively warm locations and subsequent condensation in cooler environments[3,4] which leads to enhanced concentrations at high latitudes. The upper reaches of high mountains are similar to high-latitude regions in that they too are characterized by relatively low average temperatures, but the accumulation of organochlorine compounds as a function of altitude has not yet been documented. Here we report organochlorine deposition in snow from mountain ranges in western Canada that show a 10- to 100-fold increase between 770 and 3,100 m altitude. In the case of less-volatile compounds, the observed increase by a factor of 10 is simply due to a 10-fold increase in snowfall over the altitude range of the sampling sites. In the case of the more-volatile organochlorines, cold-condensation effects further enhance the concentration of these compounds with increasing altitude. These findings demonstrate that temperate-zone mountain regions, which tend to receive**

**Table 1 Correlation between organochlorine concentrations in snow and site elevations**

| Compound | Correlation coefficient | Vapour pressure (Pa) |
|---|---|---|
| α-HCH | 0.85* | 0.1 |
| Heptachlorepoxide | 0.75* | 0.1 |
| γ-HCH | 0.73* | 0.03 |
| Dieldrin | 0.42* | 0.016 |
| Endosulphan-I | 0.76* | 0.008 |
| c-Chlordane | 0.42* | 0.003 |
| t-Chlordane | 0.34 | 0.003 |
| p p′ DDT | 0.00 | 0.0001 |
| PCBs | | |
| Σ Dichloro- | 0.54* | 0.2 (0.008–0.60) |
| Σ Trichloro- | 0.53* | 0.04 (0.003–0.022) |
| Σ Tetrachloro- | 0.00 | 0.006 (0.003–0.10) |
| Σ Pentachloro- | 0.00 | 0.001 (0.0003–0.009) |
| Σ Hexachloro- | 0.11 | 0.0002 ($7 \times 10^{-4} - 0.012$) |
| Σ Heptachloro- | 0.17 | $3 \times 10^{-4}$ ($2.7 \times 10^{-5} - 0.0015$) |

Correlation coefficients ($r$) are shown for organochlorine concentrations (ng l$^{-1}$) in snow and site elevation (m.a.s.l.) for the equation conc. $= ae^{b\,Elev.}$, where $a$ and $b$ are fitted constants. Asterisks show significance at $P \leq 0.05$, for 19 degrees of freedom. Sub-cooled liquid vapour pressures are included for pesticides at 20 °C (ref. 21) and PCBs at 25 °C (ref. 22). Published vapour pressures vary considerably, so these values represent mean reported values for all PCBs in that class. Ranges of published vapour pressures for each PCB category are shown in brackets. Only compounds with mean sample concentrations that were ten times higher than blanks were considered.

† Present addresses: Department of Biology, University of Ottawa, 30 Marie Curie Street, PO Box 450 Stn. A, Ottawa, Ontario, Canada K1N 6N5 (J.M.B.); Environment Canada, 867 Lakeshore Road, Burlington, Ontario, Canada L7R 4A6 (D.C.G.M).